For the submission to *American Journal of Physics*

Apparent Depth Observed at Oblique Angles

Tohei Moritani

Keio Academy of New York, 3 College Rd., Purchase, New York 10577

(Dated: January 1, 2018)

Abstract

The virtual image of an object in water was observed in air at oblique angles to determine the location of the image, and the data was compared with the theory of geometrical optics. Contrary to the academically accepted theoretical model in which two astigmatic virtual images exist and one of them moves closer to an observer at lower observation angles, the present work has clarified that virtual image is definitely located directly above the object at any observation angles and simply moves closer to the surface at lower observation angles. Any additional image was never observed. Similar observation and calculation was also performed using a glass plate, and the same result was obtained. Missing the astigmatic image predicted in geometrical optics can be explained by a novel idea concerning the destructive interference of out-of-phase light rays generated in the refraction process.

I. INTRODUCTION

Last summer a small article on a web newspaper drew my attention, reporting recurrent accidents by kids at swimming pools. Children misjudge the depth of water they jump into and therefore drown. The article warned that pool bottoms look much shallower than they actually are, for short kids in particular.

Apparent depth is a typical topic of optical illusions caused by the refraction of light. Many physics textbooks show photos and figures for the examples of this familiar phenomenon, such as a "bent" pencil, oar or stick, fish rising to water surface, shorter legs in water, and so on. It is well-known that the virtual image of an object in water is located at $d = D/n$, where D is the actual depth and n is the refractive index of water or 1.33, when observed in air from just above the object. In spite of its old and commonplace topic, however, the location of the virtual image observed at *oblique* angles seemed to be confused or not to be understood well, surprisingly. In many textbooks and popular scientific articles, a virtual image observed at oblique angles is depicted as being located directly above the object, the position A in Fig. 1, together with the equation $d = D/n$ which is valid only when observed above the object.

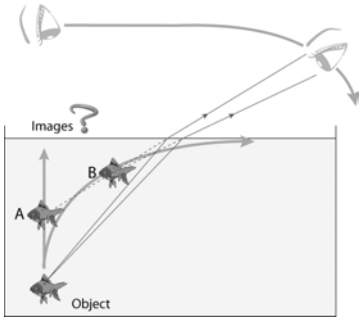

FIG. 1. Two virtual images predicted based on geometrical optics: image-A is located directly above the actual object while image-B is much shalower and closer to the observer.

In the most apparently reasonable and academically accepted model so far, two astigmatic virtual images are assumed to be formed, one each in both of the positions A and B in Fig.1. One of the images, image-B, has been rationalized based on geometrical optics and adopted as a standard model in all the related papers and books.[1-15] Theory has predicted a unique character of virtual image-B: as an observer lowers his/her angle of observation, the image becomes shallower and moves closer prominently to the observer, and the set of all possible images forms a caustic curve,[4,5,7] as shown in Fig. 1. Many papers thus adopted image-B prior to image-A probably because of the former's significant effect to make the image much shallower. Some papers exclusively adopted image-B and completely ignored image-A.[1, 5,10,12]

It has theoretically been pointed out that both of the two images, A and B, are not clearly observed simultaneously because they are assumed to have different foci, that is, the virtual images are astigmatic.[2-4,6-9,13-15] Related to the astigmatism, some papers discussed that the appearance of the two images could depend on the angles of head or the orientation of eyes, without exact experimental data.[2,3,7,8,13,15] Only two papers reported the experimental observation about the two astigmatic images. Kinsler[4] reported on the astigmatic difference between two images observed in a glass plate, where their appearance depended on observer's head orientation. Bartlett, Lucero and Johnson[9] used an object submerged in a bread pan filled with water and reported the separation of two astigmatic images. Neither paper reported the exact locations of images, only their separation. No paper includes observed data on the apparent depths in water tanks or

swimming pools although theoretical calculations were reported about apparent depth of swimming pools without showing any experimental data.[12,15]

This paper begins to formulate theory and computation methods to obtain the locations of the images-A and B from several parameters used in experiment. Next, the computed data is compared with the observed images using a water tank or using a glass plate in a separate experiment. Then, the comparison clarifies that all the observed virtual images in this work are image-A with no additional sign of the existance of image-B, contrary to the past accepted knowledge. As a conclusion, an illustration is shown to summarize the relationship between actual depth, apparent depth, observed angle and refraction point. Concerning why the image-B is missing, a hypothetical model is presented about the role of phase in refraction of light waves.

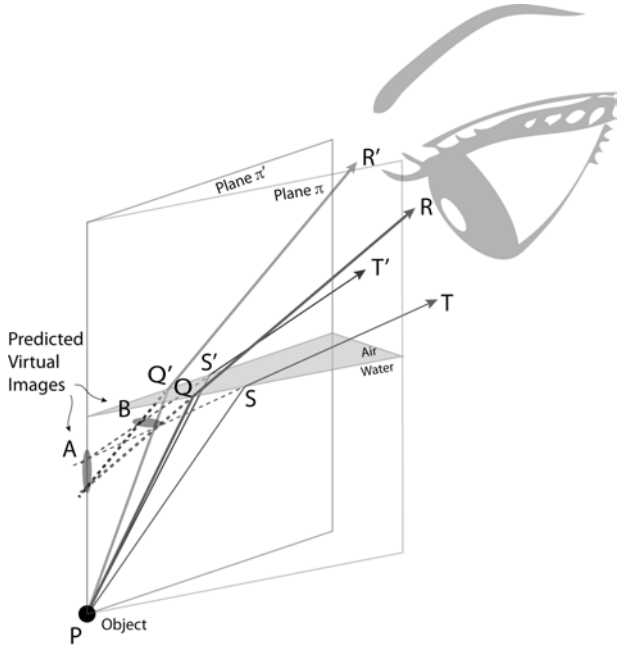

FIG. 2. Geometrical overview showing how two virtual images A and B of a point object P are formed.

II. THEORY AND COMPUTATION

II-1. Geometrical Overview Fig. 2 is an illustration in terms of geometrical optics of how virtual images are formed from a point object P in water. Light is reflected at P, and the reflected rays diverge, travel to water surface, refract there and arrive at an eye. The points, R, R', T and T', are four outer corners of the ray pencil with a size corresponding to the outer fringe of a pupil.

First, consider the pair of rays, PQR and PQ'R' having the same incident angle at water surface: PQR is on a vertical plane-π including the point object P and PQ'R' on another vertical plane-π' also including the point object P. Extending the rays, QR and Q'R', backward they intersect at a point, where we see virtual image-A, directly above the object because the intersection must be on the vertical edge of the two vertical planes. Another pair of rays, PST and PS'T' forms a similar type of image some distance above the image by QR and Q'R'. Many pairs of rays on similar two planes form images on the vertical line above P. Image-A from the point object P is thus predicted to become an extended line perpendicular to the water surface, as already stated by Sears.[6]

Next, consider the pair of rays, PQR and PST traveling on the same vertical plane-π. Extending the rays, QR and ST, backward, they intersect at a point, where we see virtual image-B, shallower and closer to the eye than image-A. Another pair of rays, PQ'R' and PS'T' forms a similar type of image some distance aside the image by QR and ST. Many pairs of rays on a plane form similar images. Image-B from the point object P is also

predicted to become an extended line parallel to the water surface, as already stated by Sears.[6]

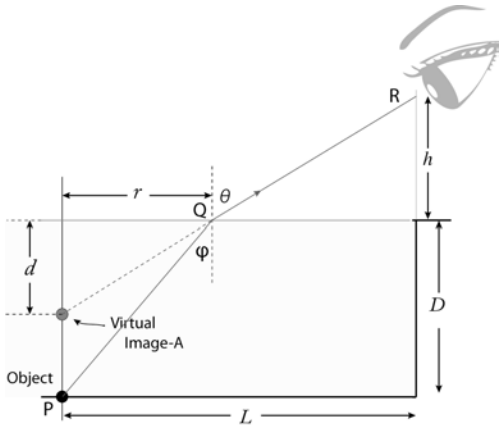

FIG. 3. The geometrical relations to obtain the location of image-A or its apparent depth *d*

II-2. Computation of Image-A

Fig. 3 shows the geometrical relations to obtain the location of image-A or its apparent depth *d* of the image formed by the rays, QR and Q'R'.

From Snell's law, $$n = \sin\theta / \sin\varphi \quad (1)$$

$$\sin\theta = r/\sqrt{r^2 + d^2}, \quad \sin\varphi = r/\sqrt{r^2 + D^2} \quad (2)$$

where D, n, θ, φ and r represent the actual depth of an object, the refractive index of water, the incident angle of light, the refractive angle and the horizontal distance between the object and the point of refraction, respectively.

From equations, (1) and (2), $n = \sqrt{r^2 + D^2}/\sqrt{r^2 + d^2}$

The squares of the both sides yield

$$d^2 = \{D^2 - (n^2 - 1) \cdot r^2\}/n^2 \quad (3)$$

Using $r = d\tan\theta$, Eq. (3) is converted to:

$$d = D/\sqrt{n^2 + (n^2 - 1) \cdot tan^2\theta} \quad (4)$$

Using the parameters, L and h in Fig.3, where L is the horizontal distance between the observer and the object while h is the height of the eye from the water surface, we obtain $\tan\theta = (L - r)/h$, and then

$$d = D/\sqrt{n^2 + (n^2 - 1) \cdot L^2/(h - d)^2} \quad (5)$$

Equation (5) is an implicit function concerning d, and hence the apparent depth d was computed using Microsoft EXCEL Goal Seek as the following manner:

INPUT data: n, L, h and D

SET CELL: $d^2 \cdot \{n^2 + (n^2 - 1) \cdot L^2/(h + d)^2\} - D^2$

To Value: 0

By Changing Cell: d

From a computed value of d, the other parameters are calculated as follows:

$$r = \sqrt{(D^2 - n^2d^2)/(n^2 - 1)}\,,\ \theta = \sin^{-1}\left(r/\sqrt{r^2 + d^2}\right),\ \varphi = \sin^{-1}\left(r/\sqrt{r^2 + D^2}\right) \quad (6)$$

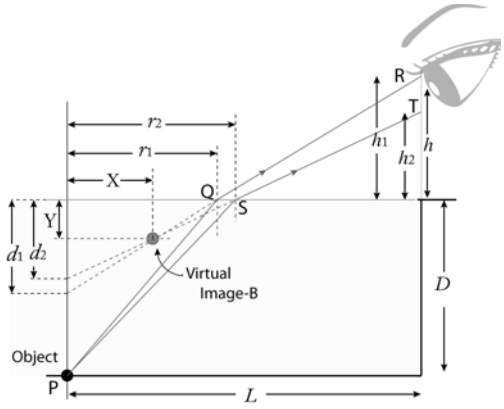

FIG. 4. Geometrical relations to obtain the location of image-B in terms of X and Y.

II-3. Computation of image-B

In Fig. 4, the location of the intersection of the rays, QR and ST, is indicated by X and Y. Computation of X and Y was performed in the following two steps:

[Step-1] When the center of the eye is h high from the water surface, the higher position of the pupil is given by $h_1 = h + \mathrm{e}/2$ and the lower by $h_2 = h - \mathrm{e}/2$ where e is the diameter of the pupil, typically 4 mm: the normal pupil size in adults varies from 2 to 4 mm in diameter in bright light to 4 to 8 mm in the dark.[16] Two geometrical parameters, d_1 and r_1, corresponding to h_1 were computed using Eqs. (5) and (6), by the same procedure based on EXCEL Goal Seek as in the calculation of Image-A. Parameters, d_2 and r_2, corresponding to h_2 were computed similarly.

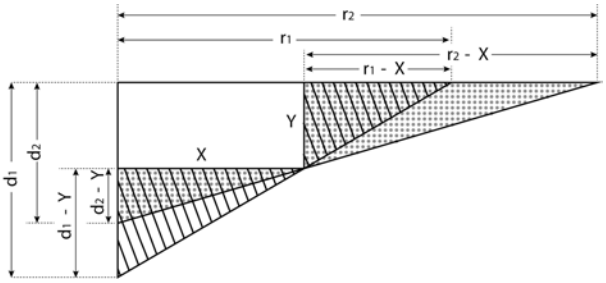

FIG. 5. Geometrical relations to obtain X and Y from d_1, r_1, d_2 and r_2.

[Step-2] Fig. 5 shows the geometrical relations among X, Y, d_1, r_1, d_2 and r_2. The two sets of similar triangles shown by dots and oblique lines give the following two relations:

$$(d_1 - Y) \,/\, Y = X \,/\, (r_1 - X), \qquad (d_2 - Y) \,/\, Y = X \,/\, (r_2 - X)$$

Solving for X and Y yields

$$X = (d_1 - d_2)/\,(d_1/r_1 - d_2/r_2), \quad Y = (r_1 - r_2)/\,(d_1/r_1 - d_2/r_2) \qquad (7)$$

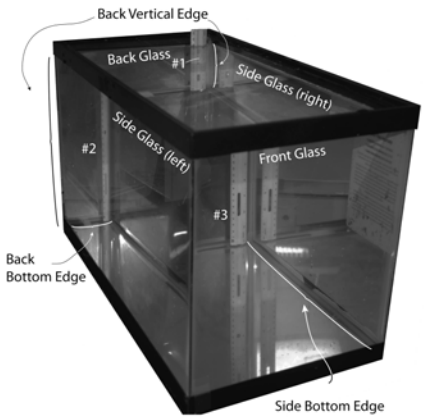

FIG. 6 The photo of the glass tank used for this experiment.

III. Comparison between Theory and Experiment

III-1. Water Tank Fig. 6 is the photo of the glass tank used for this experiment, having a dimension of 50 x 25 x 27.5 cm. In this photo, the tank is filled with water, and a 30 cm ruler is sunk and fixed against the back glass wall for demonstration. Three direct virtual images are seen in this photo: #1 is the image formed in the refraction at the upper water surface, #2 is formed at the left side surface and #3 is formed at the front surface. In this photo, additional nine reflected images of the virtual images are also seen.

III-2. Observation from above the tank The water tank was observed from above to determine the apparent depth of the bottom of the back glass for the various height of an eye, h. The measurement was performed with a ruler fixed outside the tank. The observed and theoretical results are shown in Table I. The observed apparent depths agree well with the theoretical values for image-A and clearly not for image-B. Fig. 7 is depicted based on the theortecal calculation for two cases, h = 10 and 20 cm. Narrow solid lines indicate the rays emerged from major locations on the edges while narrow

dashed lines extended lines of the refracted rays backward. The image-A of the back vertical edge is drawn as a bold black line overlapped with the actual edge while the image-B of the back vertical edge is drawn as a bold gray curve line much shallower and closer to the observer than the image-A. The observed virtual images distinctly agree with the theoretical image-A and completely differ from the theoretical image-B. Thus, it has been concluded that the observed image is image-A , and no image-B exists in this observation.

Table I Observed and theoretical values of the virtual images for the bottom of back glass, viewed from above the water tank. (The depth of an actual object: $D = 27.5$ cm)

Height of an eye (cm)	Depth of the image for the bottom of the back glass (cm)			
	Observed	Theoretical		
h	*d*	Image-A	Image-B	
		d	Y	X
2	3.8	3.3	0.09	30
3	5.1	4.7	0.24	29
4	6.2	6.0	0.51	27
5	7.1	7.2	0.85	26
7.5	10.4	9.5	2.0	22
10	12.0	11.2	3.3	19
15	14.0	13.5	5.8	14
20	15.8	15.1	8.2	10

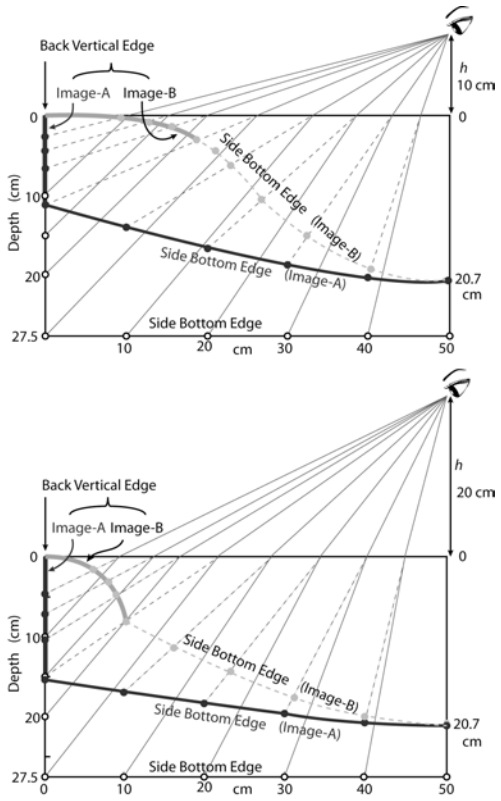

FIG. 7. Theoretical images, A and B, of the back vertical and side bottom edges viewed from above the water tank for two cases, h = 10 and 20 cm.

Table II Observed and theoretical values of the virtual images for the right side bottom edge, viewed from left side. (The depth of an actual object: D = 25 cm)

Distance of an eye (cm)	Depth of the image for the side bottom edge (cm)			
h	Observed	Theoretical		
	d	Image-A	Image-B	
		d	Y	X
2	3	2.6	0.050	28
3	4	3.8	0.15	27
4	5	4.9	0.33	26
5	6	5.9	0.58	24
7.5	8	8.0	1.5	21
10	9	9.6	2.5	18
15	12	12	4.7	13
20	14	13	6.8	9.9

III-3. Observation from the side of the tank The water tank was observed from left side to determine the apparent depth of right side bottom edge for the various distance of an eye, h. The observed and theoretical results are shown in Table II. The observed apparent depths agree well with the theoretical values for image-A and clearly not for image-B. Fig. 8 shows the theortecal calculation. The image-A of the back bottom edge is drawn as a bold black line overlapped with the actual edge while the image-B of the back bottom edge is drawn as a bold gray curve line much shallower and closer to the observer than the image-A. The observed virtual images distinctly agree with the theoretical image-A and completely differ from the theoretical image-B. This can be confirmed visually by comparing Fig. 8 with Fig. 6. Thus, it has also been concluded that the observed image is image-A, and no image-B exists in this observation.

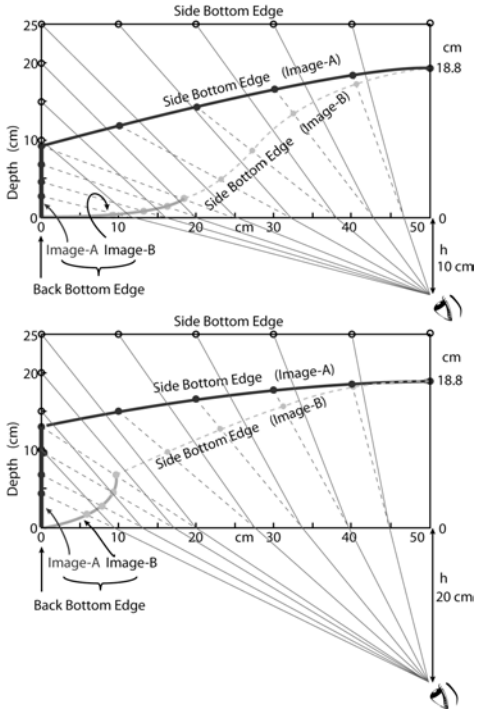

FIG. 8. The theoretical images, A and B, of the back bottom and side bottom edges viewed from the side of the water tank for two cases, h = 10 and 20 cm.

III-4. Observation from the side of a glass plate Besides the tank experiment, an additional and different experiment was performed using a glass plate with a dimension of 20.3 x 27.9 x 1.25 cm and refractive index of 1.52, as shown in Fig. 9. A red LED was placed at a back corner of the plate and the virtual image of the LED was observed from front side. The lengths, r and d were measured for various locations of an eye. Theoretical calculations were also performed by a method similar to the water tank. The results are shown in Table III. The observation agrees well with the theoretical values for image-A and clearly not for image-B. Thus, it has also been concluded that the observed image is image-A, and no image-B exists in this observation.

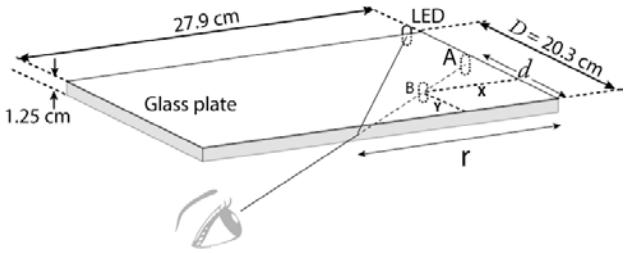

FIG. 9. A glass plate equipped with a red LED and the observation of its virtual image.

Table III Observed and theoretical values of virtual images of a red LED viewed from the front side of a glass plate. (The depth of an actual object: D = 20.3 cm)

Location of refraction (cm)	Depth of LED image (cm)			
r	Observed	Theoretical		
	d	Image-A	Image-B	
		d	Y	X
4	14	13.0	12.3	0.204
6	13	12.6	11.1	0.687
8	12.5	11.9	9.49	1.63
10	11.4	11.0	7.52	3.18
12	9.8	9.8	5.33	5.50
14	8.9	8.2	3.09	8.73
16	6.3	5.8	1.07	13.0

III-5. Orientation of eyes Several papers[2,3,7,8,13,15] suggested that the appearance of virtual images in water depends on the orientation of eyes, " head erect" or "head tilted 90° ." In this experiment, however, no difference was observed in the intensity, appearace or location of image-A depending on the orientation of eyes or between single-eye and two-eyes observations. Image-B predicted in geometircal optics was never observed in any orientation of eyes.

III-6. Aberration of a virtual image Theory of geometrical optics predicts aberration of a virtual image, that is, the virtual image of a point object P in Fig. 2 does not have a clear focus but forms an extended line perpendicular to water surface, as stated in II-1. The length of the line was theoretically calculated as $\Delta d = d_1 - d_2$ indicated in Fig. 4, and some calculation results are summarized in Table IV. The values of Δd and the ratio of abberation, $\frac{\Delta d}{d_1} \times 100$, are 0.13 to 0.86 cm and 0.86 to 11.4%, respectively, under the conditions of this tank experiment. This aberration was not experimentally deteced, however, probably due to their small effect.

Table IV Theoretical calculation results showing the length of extended line image from a point object.

Diameter of a pupil	[cm]	e	0.5	0.5	0.5	0.8
Height of an eye	[cm]	h	20	10	5	5
Depth of a water tank	[cm]	D	50	50	50	50
Apparent depth -1	[cm]	d_1	15.13	11.32	7.42	7.57
Apparent depth -2	[cm]	d_2	15.00	11.02	6.88	6.71
Length of the virtual image	[cm]	$\Delta d = d_1 - d_2$	0.13	0.30	0.54	0.86
Ratio of abberation	[%]	$\frac{\Delta d}{d_1} \times 100$	0.83	2.63	7.25	11.4

IV. Discussion

IV-1. Image-A The virtual images observed in this experiment were definitely located directly above the object in case of the observation from above (located on the line normal to surface from the actual object in case of the observation from the side) when observed at any angle, and simply moves closer to surface at lower observation angles. By comparison with the computation based on the geometrical optics, all the virtual images in the present experiments have been concluded as image-A.

IV-2. Image-B Image-B, adopted as the proper model in all of the papers on apparent depth before this work, was never found in the present work. Desperate search was conducted to find image-B using optical devices such as a camera and a microscope because the theoretical model was regarded as reasonable, the invisibleness seemed rather curious, there could be a possibility to be “hidden” in front of image-A, and above all else

two papers[4,9] reported the existance of two astigmatic images experimentally. In the present work, however, all of the efforts to find image-B were wasted and it has been concluded finally that image-B does not exist in this experiments.

IV-3. Astigmatism In Sear's textbook,[6] he showed a geometrical drawing and explained how two astigmatic images of a point object were formed by refraction. By the word of "astigmatic," he seemed to mean two properties. First, two images with diferrent foci must be formed, and secondly the two images formed from a point object result in mutually perpendicular extended lines, not points. One of the two images, image-B, was never observed here. While, on the other hand, the latter can be expected theoretically, as stated in III-6, and calculated result is shown in Table IV, although no abberation was detected experimentally due to its small effect.

VI-4. Apparent Depth Observed at Oblique Angles Fig. 10 shows an illustration summarizing the relationship among the apparent depth d of a point object located at D =1.00 m deep in water, observation angle θ in air expressed as the angle of refraction and refraction point r from the object. Calculation was performed using the equations (4) and (6), as also shown in the figure. The virtual image is definitely located directly above the actual object, and does not move sideways. The ratio d/D is 0.752 or $1/n$, 0.495 and 0.194 at $\theta = 0^\circ$,60° , 80° , respectively.

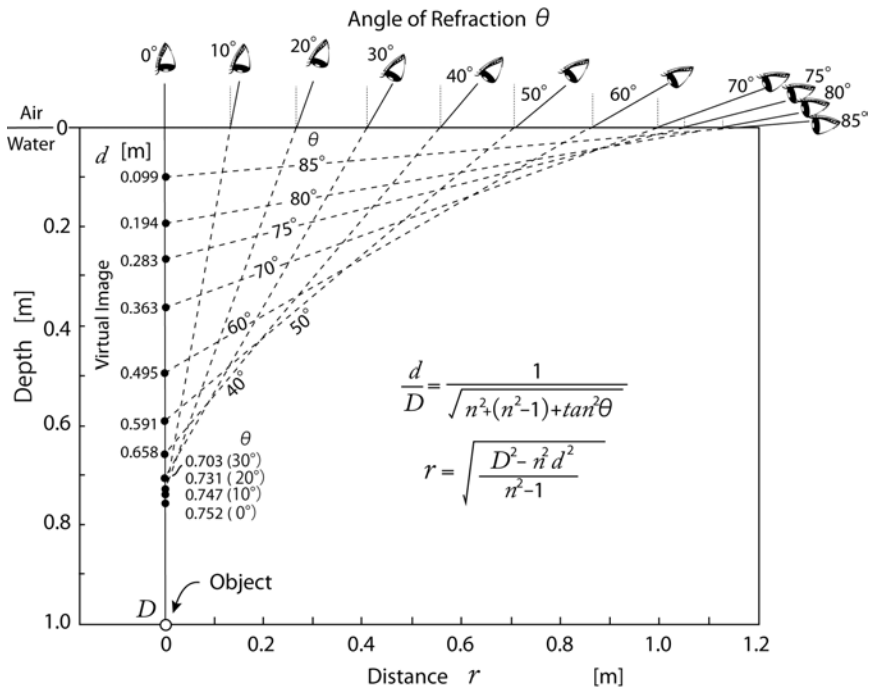

FIG. 10. Apparent depth of virtual image in water. The object is located at D =1.00 m deep. The graph shows the relations among apparent depth d, the angle of refraction θ and horizontal distance r between the object and refraction point. The parameter n represents the refraction index of water or 1.33.

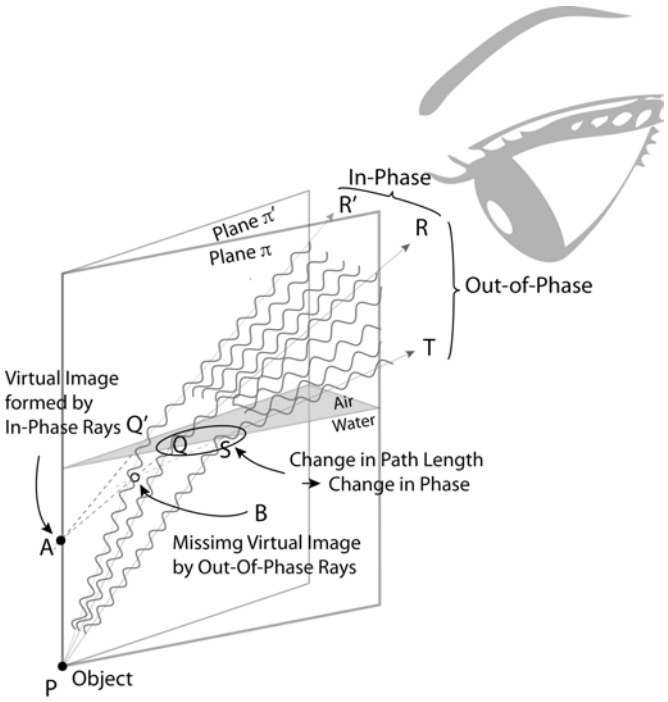

FIG. 11. A hypothetical model showing the behavior of phase in light waves at refraction. The pencil of rays forming image-A is in-phase while that forming image-B is out-of-phase causing destructive interference. The latter can be the reason of missing image-B.

VI-5. Missing Image and Wave Optics on Refraction The invisibility of perpendicular image-B in this experiment naturally encouraged the author to find theoretical reasoning and finally brought him to consider wave optics on refraction and notice the role of phase in light waves in particular.

Fig. 11 shows a novel hypothetical model concerning the behavior of phase of light at the refraction of rays. As the first approximation in this model, the light emerging at an object in water is assumed to be perfectly simple, that is, the light is a continuous wave having single frequency, amplitude, phase and polarization angle, or a completely *coherent* wave. Although the real light is not that ideal, the beams originating in the

same sauce are in general correlated or *partially coherent*,[17,18] and then the present model is assumed to work as follows.

The light emerging at the object travels from water into air and the wavelengh changes 1.33 times longer. In the formation of image-A, the relevant rays, all the rays between the rays PQR and PQ'R' in the figure, are all in almost in-phase because they travels on optical paths with the identical, or almost identical length. On the contrary, in the formation of image–B, the relevant rays, all the rays between PQR and PST in the figure, travel on optical paths whose length in water changes depending on refraction point from Q to S. Changing the length of optical path affects the phase of waves in air.

Fig. 12 shows this situation more in detail. The diagonal line in this figure represents a water surface. From its left side, parallel and in-phase light waves travel in water, enter into air at the surface and then change their wavelength according to the difference of indices of refraction, 1.33 times longer. The series of waves are passing through the surface *obliquely*, hence the length of optical path in water is changing one after another, and suceedingly the extention of wavelength in air is starting at various phases in waves, as shown. Consequently, the resultant series of light waves are in out-of-phase each other and can interfere destructively, and therefore image-B is not formed. Fig. 11 intentionally illustrates waves travelling parallel and passing straight across an oblique water surface instead of waves diverging radiantly from an object and bending at refraction because the latter effects are not essential in the generation of the out-of-phase pencil of light.

The relationship between phase in waves and its distribution is shown more directly in Fig. 13, showing schematically the cross-section of rays in the vicinity of a pupil. The

square represents the range of a pupil and corresponds to RR'TT'in Fig. 2 and 10. Circles inside the square represent light waves that have different phases denoted by different colors: corresponding typical phases are shown in the right side. As the result of refraction, the series of rays placed in row paralell to water surface becomes in-phase while the series of rays placed in column perpendicular to water surface becomes out-of-phase. These series of rays enter into an eye through a crystaline lens and form an image on a retina. During this process the rays combine and interfere each other in accordance with the superposition principle. The combination of the rays placed in the column fails to form virtual image-B due to destractive interference while the combination of the rays placed in the row successfully froms image-A.

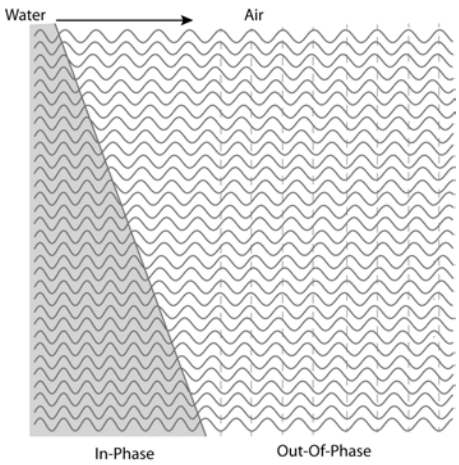

FIG. 12. Generating out-of-phase waves in refraction. In-phase light waves traveling in water from left arrive at an oblique water-air interface, Q-R, pass it through and extend their wavelength in air. As the path length of the incident light is changing, the extended waves in air are also changing their phase one after another, resulting in the formation of

series of out-of-phase waves on the perpendicular line of a pupil, R-T. These out-of-phase waves, interfering each other destructively, cannot make a role to form image-B.

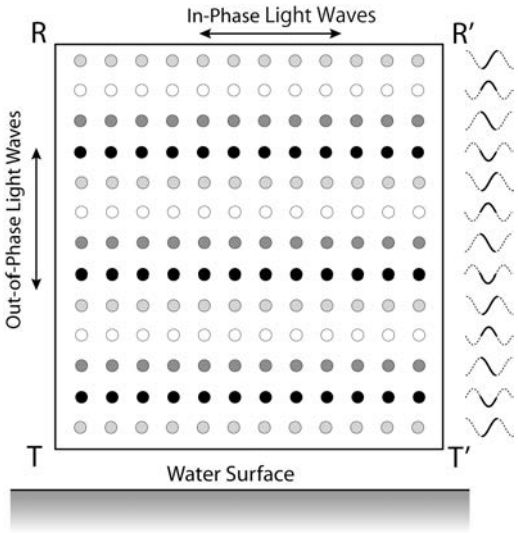

FIG. 13 Phase distribution in refracted waves is shown schematically for the cross-section of pencil of rays in the vicinity of a pupil. The square corresponds to RR'TT' in Figs. 2 and 10, and the circles represent light waves with phases denoted by different colors corresponding to typical wave forms. As the result of refraction, the series of rays in row becomes in-phase while the series in column becomes out-of-phase. The combination of the latter series fails to form image-B due to destructive interference while that of the former rays successfully forms image-A.

Acknowledgment

The author is thankful to the management of Keio Academy of New York for giving him this opportunity of the work.

---

* tmoritani@mac.com

[1] E. R. Laird, "The Position of the Image of an Object Under Water," Am. J. Phys. **6** (1), 40 (1938); " Response to "Where is a Fish Seen?'," Am. J. Phys. **6** (3), 164 (1938).

[2] H. M. Reese, "Where is a Fish Seen?," Am. J. Phys. **6** (3) 163 (1938).

[3] G. Arvidsson, "Image of an Object Under Water," Am. J. Phys. **6** (3) 164 (1938).

[4] L. E. Kinsler, "Imaging of Underwater Objects," Am. J. Phys. **13** (4) 255-257 (1945).

[5] F. A. Jenkins and H. E. White, *Fundamentals of Optics*, 4th edition (McGraw-Hill Book Co., New York, NY, 1976), pp. 36-40.

[6] F. W. Sears*, Optics*, (Addison-Wesley Publishing Company, Inc., Reading, MA, 1949), pp. 39-43.

[7] A. V. Barz, "Apparent Depth and the Virtual Caustic," Am. J. Phys. **14** (4) 45-47 (1946).

[8] J. F. Goehl, Jr., "Investigation of the variation of apparent depth with viewing angle by ray tracing," Am. J. Phys. **45** (10) 999 (1977).

[9] A. A. Bartlet, R. Lucero and G. O. Johnson, "Note on a common virtual image," Am. J. Phys. **52** (7) 640-643 (1984).

[10] M. Svonavec, "Problem: Fermat's Principle Extended by Virtual Optical Path," Am. J. Phys. **53** (2) 181,185 (1985).

[11] J. F. Goehl, Jr., "Astigmatism and Apparent Depth," Am. J. Phys. **53** (11) 1037 (1985).

[12] A. B. Nassar, "Apparent Depth," Phys. Teach. **32** (9) 526-529 (1994).

[13] A. A. Bartlett, "The article "Apparent Depth'," Phys. Teach. **33** (4) 199 (1995).

[14] E. Mosca, "A.B. Nassar considered the question: As viewed from an arbitrary angle, how far beneath the surface of the water of a swimming pool does an object at depth D appear to be?," Phys. Teach. **33** (4) 199 (1995).

[15] K. S. Mendelson, "Apparent shape of a swimming pool," Phys. Teach. **78** (12) 1254-1257 (2010).

[16] H. K. Walker, W. D. Hall and J. W. Hurst, *Clinical Methods: The History, Physical, and Laboratory Examinations,* 3rd edition (Butterworths, Boston, MA 1990); https://www.ncbi.nlm.nih.gov/books/NBK381/

[17] M. Born and E. Wolf, *Principles of Optics*, 7th (Expanded) edition(Cambridge University Press, Cambridge, UK, 1999), p286.

[18] E. Hecht and A. R. Ganesan, *Optics*, 4th edition (Pearson, Chennai, India, 2008), pp. 370-372.